References

[1] N. Marcuvitz, *Waveguide Handbook*. Radiation Laboratory Series, vol. 10. New York: McGraw-Hill, 1951.

[2] S. O. Rice, "Reflection from corners in rectangular waveguides—conformal transformation," *Bell Sys. Tech. J.*, vol. 28, pp. 104–135.

[3] S. O. Rice, "A set of second order differential equations associated with reflections in rectangular waveguides," *Bell Sys. Tech. J.*, vol. 28, pp. 136–156, January 1949.

[4] J. J. Campbell, "Application of the solutions of certain boundary value problems to the symmetrical four-port junction and specially truncated bends in parallel-plate waveguides and balanced strip-transmission lines," *IEEE Trans. Microwave Theory and Techniques*, vol. MTT-16, pp. 165–176, March 1968.

[5] S. A. Schelkunoff, "Conversion of Maxwell's equations into generalized telegraphists' equations," *Bell Syst. Tech. J.*, vol. 34, pp. 995–1043, September 1955.

[6] E. A. Coddington and N. Levinson, *Theory of Ordinary Differential Equations*. New York: McGraw-Hill, 1955.

[7] J. W. Miles, "The equivalent circuit for a plane discontinuity in a cylindrical waveguide," *Proc. IRE*, vol. 34, pp. 728–742, October 1946.

Variational Method for the Analysis of Microstrip-Like Transmission Lines

EIKICHI YAMASHITA, MEMBER, IEEE

Abstract—**A theoretical method is presented by which microstrip-like transmission lines can be analyzed. These transmission lines are characterized by conducting strips, large ground planes, multi-dielectric-layer insulation, and planar geometry. The method is essentially based on a variational calculation of the line capacitance in the Fourier-transformed domain and on the charge density distribution as a trial function. A shielded double-layer microstrip line is analyzed by this method. Derived formulas for this structure are also applicable to simpler structures: a double-layer microstrip line, a shielded microstrip line, and a microstrip line. The calculated values of the line capacitance and the guide wavelength are compared with the measured values where possible. Oxide-layer effects on a silicon microstrip line and shielding effects on a sapphire microstrip line are also discussed based on this theory. The limitations and possible applications of this method are described.**

I. Introduction

MICROSTRIP-LIKE transmission lines have been widely discussed recently in connection with the microwave integrated circuitry. These transmission lines are characterized by conducting strips, large ground planes, multi-dielectric-layer insulation, and planar geometry. It is, therefore, desirable to develop a general design theory which covers all transmission lines of this type.

The microstrip line is a simple structure mechanically and has been known for more than a decade. Yet it had not been analyzed with reasonable accuracy until a modified conformal mapping [1], a relaxation method [2], and a variational method [3] were investigated. The theoretical difficulty of this structure is attributed to the dielectric boundary conditions restricting electric fields. The above variational method for the microstrip line [3] treats the dielectric boundary conditions in a general way so that a multi-layer microstrip line can be analyzed without difficulty.

Manuscript received November 17, 1967; revised March 11, 1968. The work reported here was supported by U. S. Army Research Grant DA-G-646.

The author was with the Antenna Laboratory, Department of Electrical Engineering, University of Illinois, Urbana. He is now with the University of Electro-Communications, Tokyo, Japan.

In the microwave integrated circuit applications, the following modifications of the microstrip line are useful: a shielded (packaged) microstrip line, the oxide film coating of substrate [4], the glazing of alumina substrate [5], and an integrated circuit supported between two parallel ground planes. The last example is also a modification of an integrated circuit mounted in a coaxial structure [6].

This paper applies the above variational method [3] to a shielded double-layer microstrip line. Derived formulas for this structure are also applied to simpler structures, a double-layer microstrip line, a shielded microstrip line, and a microstrip line, by substituting appropriate structural parameters. The calculated values of the characteristic impedance and the guide wavelength are compared with the measured values where possible. Oxide-layer effects on a silicon-substrate microstrip line and shielding effects on a sapphire-substrate microstrip line are discussed based on this theory. Finally, possible applications and limitations of this method are described.

II. Shielded Double-Layer Microstrip Line

A transmission line as shown in Fig. 1 has the line capacitance C. Suppose all the dielectric layers are removed from this structure. The remaining conductor system has the line capacitance C_0, which is smaller than C. The theory of a distributed-parameter transmission line gives a relation between the wavelength of an unloaded line λ_0 and the guide wavelength of a capacitance-loaded line λ.

$$\lambda = \left(\frac{C_0}{C}\right)^{1/2} \lambda_0. \tag{1}$$

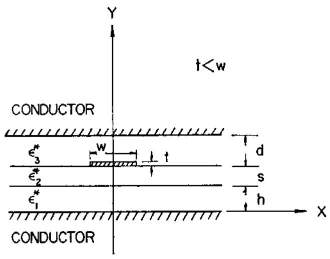

Fig. 1. Shielded double-layer microstrip line.

Similarly, it gives a relation between the characteristic impedance of the unloaded line Z_0 and the characteristic impedance of the capacitance-loaded line Z:

$$Z = \left(\frac{C_0}{C}\right)^{1/2} Z_0. \tag{2}$$

As is well known in the TEM transmission theory, λ_0 is identical to the free-space wavelength, and Z_0 is given by

$$Z_0 = \frac{1}{C_0 c} \tag{3}$$

where c is the velocity of light.

In this paper, the line capacitance is formulated as a variational integral in the Fourier-transformed coordinate. The processes of deriving the line capacitance formula are as follows.

1) Since the distributed capacitance is concerned here, the static theory can be used to calculate it. The potential distribution $\phi(x, y)$ in the cross-sectional area of the line is ruled by Poisson's equation

$$\nabla^2\phi(x, y) = -\frac{1}{\epsilon}\rho(x, y) \tag{4}$$

where $\rho(x, y)$ is the charge density distribution and ϵ is the permittivity.

2) A spacing of the dimension p is made between the strip conductor and the dielectric sheet.[1] Then the charge density on this infinitely thin strip is expressed as

$$\rho(x, y) = \delta(y - h - s - p) f(x) \tag{5}$$

where $\delta(y-h-s-p)$ is Dirac's delta function.

3) The Fourier transform is applied to all field quantities like

$$\tilde{f}(\beta) = \int_{-\infty}^{\infty} f(x) e^{j\beta x} dx. \tag{6}$$

[1] The original structure is expressed as the limit $p \rightarrow 0$ after applying boundary conditions. This artifice is to be convenient for separating the dielectric boundary condition and the continuity conditions at $y = h+s$, and, hence, for matching the number of equations to the number of unknown variables.

4) Then Poisson's equation is rewritten as

$$\left(\frac{d^2}{dy^2} - \beta^2\right)\tilde{\phi}(\beta, y) = 0 \quad (y \neq h,\ h+s,\ h+s+p). \tag{7}$$

The general solution of this differential equation is a linear combination of $\exp(\beta y)$ and $\exp(-\beta y)$ in a bounded region. When d is taken as infinity, the solution takes a form of $\exp(-|\beta| y)$ in the unbounded region.

5) The boundary conditions and continuity condition of this structure are given as follows:

$$\tilde{\phi}(\beta, 0) = 0 \tag{8a}$$

$$\tilde{\phi}(\beta, h + s + d) = 0 \tag{8b}$$

$$\tilde{\phi}(\beta, h + 0) = \tilde{\phi}(\beta, h - 0) \tag{8c}$$

$$\epsilon_2^* \frac{d}{dy}\tilde{\phi}(\beta, h + 0) = \epsilon_1^* \frac{d}{dy}\tilde{\phi}(\beta, h - 0) \tag{8d}$$

$$\tilde{\phi}(\beta, h + s + 0) = \tilde{\phi}(\beta, h + s - 0) \tag{8e}$$

$$\epsilon_3^* \frac{d}{dy}\tilde{\phi}(\beta, h + s + 0) = \epsilon_2^* \frac{d}{dy}\tilde{\phi}(\beta, h + s - 0) \tag{8f}$$

$$\tilde{\phi}(\beta, h + s + p + 0) = \tilde{\phi}(\beta, h + s + p - 0) \tag{8g}$$

$$\frac{d}{dy}\tilde{\phi}(\beta, h + s + p + 0) = \frac{d}{dy}\tilde{\phi}(\beta, h + s + p - 0) - \frac{1}{\epsilon_3^*\epsilon_0}\tilde{f}(\beta) \tag{8h}$$

where ϵ_1^*, ϵ_2^*, and ϵ_3^* are the relative dielectric constants. When more dielectric layers are involved, more boundary conditions have to be added in a similar fashion. It is noted that since the structure is symmetrical, $f(x)$ and $\tilde{f}(\beta)$ are also symmetrical.

6) Substituting these conditions to the general solution, one obtains a set of linear inhomogeneous simultaneous equations for the coefficients of potential functions. Now the spacing p is taken as zero so as to go back to the original structure. Then the solution of the potential distribution on the strip is

$$\tilde{\phi}(\beta, h + s) = \frac{1}{\epsilon_0}\tilde{f}(\beta)\tilde{g}(\beta) \tag{9}$$

where

$$\tilde{g}(\beta) = \frac{\epsilon_1^* \coth(|\beta| h) + \epsilon_2^* \coth(|\beta| s)}{|\beta| \left\{\epsilon_1^* \coth(|\beta| h)[\epsilon_3^* \coth(|\beta| d) + \epsilon_2^* \coth(|\beta| s)] + \epsilon_2^*[\epsilon_2^* + \epsilon_3^* \coth(|\beta| d) \coth(|\beta| s)]\right\}} \tag{10}$$

ϵ_0 is the permittivity of vacuum, and parameters in this expression are defined in Fig. 1.

7) The variational expression of the line capacitance in the x coordinate [7] is given by

$$\frac{1}{C} = \frac{1}{Q^2}\int_{-\infty}^{\infty} f(x)\phi(x, h + s) dx \tag{11}$$

where

$$Q \equiv \int_{-\infty}^{\infty} f(x)dx. \tag{12}$$

The expression (11) is converted to the one in the β coordinate by using Parseval's formula [8]. The result is

$$\frac{1}{C} = \frac{1}{2\pi Q^2}\int_{-\infty}^{\infty} \tilde{f}(\beta)\tilde{\phi}(\beta, h + s)d\beta. \tag{13}$$

The formula (13) is more convenient than (11), because the process of the inverse Fourier transform is unnecessary.

8) So far, only an infinitely thin strip has been considered. However, one can approximately take into account the strip thickness t by considering the potential distribution at $y=h+s+t$. Since there is a relation which is found in the above analytical processes

$$\tilde{\phi}(\beta, h + s + t) = \frac{\sin h(|\beta| d - |\beta| t)}{\sin h(|\beta| d)}\tilde{\phi}(\beta, h + s) \tag{14}$$

the line capacitance should be written in the form

$$\frac{1}{C} = \frac{1}{2\pi Q^2}\int_{-\infty}^{\infty} \tilde{f}(\beta)\tilde{\phi}(\beta, h + s)\tilde{h}(\beta)d\beta \tag{15}$$

where

$$\tilde{h}(\beta) \equiv \frac{1}{2}\left\{1 + \frac{\sin h(|\beta| d - |\beta| t)}{\sin h(|\beta| d)}\right\}. \tag{16}$$

The final form of the line capacitance including the strip thickness is, therefore,

$$\frac{1}{C} = \frac{1}{\pi Q^2 \epsilon_0}\int_{0}^{\infty} \{\tilde{f}(\beta)\}^2 \tilde{g}(\beta)\tilde{h}(\beta)d\beta. \tag{17}$$

9) The charge density distribution is properly chosen as discussed in the following section, and the line capacitance integral is numerically evaluated. C_0 is computed simply by substituting $\epsilon_1^* = \epsilon_2^* = \epsilon_3^* = 1$ in (17).

III. Charge Density Distribution

Since the charge density distribution $f(x)$ is still unknown, one has to find a reasonable trial function. The charge density on an infinitely thin conductor strip in free space has been calculated based on the electrostatic theory [9], and the solution indicates the rapid increase of the charge density near the edge of the strip, namely,

$$f(x) = \begin{cases} \left(1 - \left(\dfrac{2x}{w}\right)^2\right)^{-\frac{1}{2}} & \left(-\dfrac{w}{2} \leqq x \leqq \dfrac{w}{2}\right) \\ 0 & (\text{otherwise}) \end{cases} \tag{18}$$

where w is the strip width. Dukes also observed a similar distribution in his experiment on a homogeneous strip line [10].

For the microstrip line, it would, therefore, be natural to assume a trial function of this type. It is an advantage of the variational expression that the accuracy of the calculated value is relatively insensitive to the choice of the trial function. Besides, the approximate line capacitance obtained by this method is always smaller than the exact value. Therefore, one can use, as a criterion for choosing a trial function, that a trial function resulting in a larger line capacitance is a better trial function.

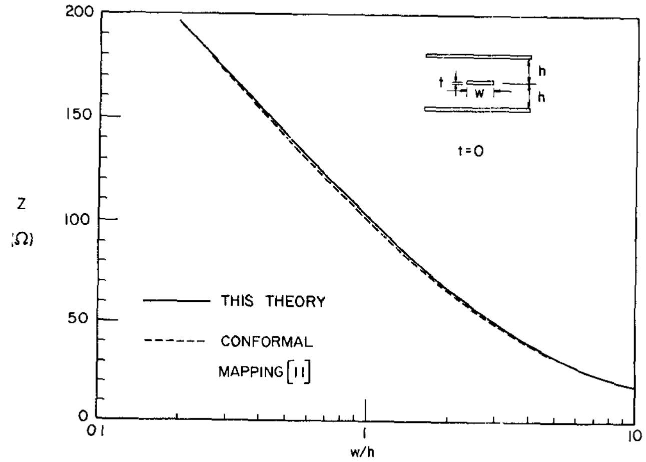

Fig. 2. Comparison of this theory with a conformal mapping in a special case.

The charge distribution (18) is approximated by a series

$$f(x) = \begin{cases} A_0 + A_1|x| + A_2x^2 + \cdots & \left(-\dfrac{w}{2} \leqq x \leqq \dfrac{w}{2}\right) \\ 0 & (\text{otherwise.}) \end{cases} \tag{19}$$

When a finite series is chosen, the coefficients of the series should be adjusted so as to obtain the maximum value of the line capacitance. The microstrip line calculation [3] shows that even a simple function, $f(x) = |x|$, gives the line capacitance with good accuracy. Taking many more terms than this trial function, one could calculate the capacitance more accurately, although more computing time would be necessary. A compromise between the computing time and the accuracy should be made in practice.

We tested a trial function,

$$f(x) = \begin{cases} 1 + A\left|\dfrac{2x}{w}\right|^3 & \left(-\dfrac{w}{2} \leqq x \leqq \dfrac{w}{2}\right) \\ 0 & (\text{otherwise}) \end{cases} \tag{20}$$

for various structural parameters. As a result, it was found that the trial function (20) is slightly better than $f(x) = |x|$ when $A = 1$. Then the Fourier transform of $f(x)$ is readily given by

$$\begin{aligned} \frac{\tilde{f}(\beta)}{Q} = \frac{8}{5}\left\{\frac{\sin(\beta w/2)}{\beta w/2}\right\} &+ \frac{12}{5(\beta w/2)^2} \\ \cdot \left\{\cos(\beta w/2) - \frac{2\sin(\beta w/2)}{\beta w/2} \right.&\left.+ \frac{\sin^2(\beta w/4)}{(\beta w/4)^2}\right\}. \end{aligned} \tag{21}$$

This is a rapidly decreasing function of βw. Consequently, the line capacitance integral converges fast.

A special case is considered for comparison with the other theory:

$$\epsilon_1^* = \epsilon_2^* = \epsilon_3^* = 1$$
$$d = h + s \qquad t = 0.$$

Then the structure in Fig. 1 becomes identical to a triplate strip line. The calculated values of the characteristic impedance by this theory and a conformal mapping [11] are shown in Fig. 2. The good agreement between these two theories supports this choice of the charge density distribution.

IV. Experiments on Shielded Double-Layer Microstrip Line

An experimental line was constructed which consists of a copper strip electroplated on a polystyrene sheet and two brass ground-planes as shown in Fig. 1. The parameters of the line were

$$\epsilon_1{}^* = \epsilon_3{}^* = 1 \qquad \epsilon_2{}^* = 2.55 \text{ (polystyrene)}$$
$$w = 5.20 \text{ mm} \qquad t = 0.20 \text{ mm}$$
$$s = 4.90 \text{ mm} \qquad h = 3.05 \text{ mm}.$$

The width of the ground plane was 200 mm. The height of the upper ground plane d was chosen as a variable in experiment, and the line capacitance at 1.5 MHz and the guide wavelength at 4 GHz were measured. The calculation of the line capacitance and the guide wavelength were carried out by the IBM 7094 computer. The computing time of the capacitance integral for one structure was less than ten seconds (GO TIME). Figs. 3 and 4 show the measured and calculated values. Agreement seems good enough to proceed with further investigation.

V. Shielded Microstrip Line

A shielded microstrip line, as shown in Fig. 5, corresponds to a special case ($s=0$) of the structure in Fig. 1. Accordingly, the formula of $\tilde{g}(\beta)$ is reduced to

$$\tilde{g}(\beta) = \frac{1}{|\beta| \{\epsilon_1{}^* \coth(|\beta| h) + \epsilon_3{}^* \coth(|\beta| d)\}}. \tag{22}$$

Substituting (16), (21), and (22) in (17), one can evaluate the line capacitance.

The shielding effects of a sapphire microstrip line [12] are considered here as an example case:

$$\epsilon_1{}^* = 9.9 \text{ (sapphire)} \qquad \epsilon_3{}^* = 1$$
$$d/h = 1, 2, 5$$
$$t/h = 0, 0.02$$
$$w/h = 0.1 \sim 10$$

The calculated values of the characteristic impedance and the guide wavelength are shown in Figs. 6, 7, 8, and 9. It is apparent from these results that the effect of shielding is almost negligible when d/h is more than 5. The effect is also larger for a wider strip.

VI. Double-Layer Microstrip Line

A double-layer microstrip line, as shown in Fig. 10, is a special case ($d\to\infty$, $\epsilon_3{}^*=1$) of the structure in Fig. 1. Therefore, $\tilde{g}(\beta)$ and $\tilde{h}(\beta)$ are reduced to:

$$\tilde{g}(\beta) = \frac{\epsilon_1{}^* \coth(|\beta| h) + \epsilon_2{}^* \coth(|\beta| s)}{|\beta| \{\epsilon_1{}^* \coth(|\beta| h)[1 + \epsilon_2{}^* \coth(|\beta| s)] + \epsilon_2{}^*[\epsilon_2{}^* + \coth(|\beta| s)]\}} \tag{23}$$

and

$$\tilde{h}(\beta) = \tfrac{1}{2}\{1 + \exp(-|\beta| t)\}. \tag{24}$$

The line capacitance is obtained by substituting (21), (23), and (24) in (17).

An experiment was carried out by removing the upper ground plane of the shielded double-layer microstrip line in Section IV. The height h was experimentally varied as multiple values of $h_0=3.05$ mm. The calculated and measured values are shown in Figs. 11 and 12.

Similarly, oxide-layer effects on a silicon microstrip line [4] can be analyzed. In this case

$$\epsilon_1{}^* = 12 \quad \text{(Si)}$$
$$\epsilon_2{}^* = 4.5 \quad \text{(SiO)} \quad [4].$$

The change of transmission properties are estimated as shown in Figs. 13, 14, 15, and 16. Two concrete examples are considered from these results:

1) $h = 125$ microns $\quad s = 1.25$ microns
$w = 12.5$ microns $\quad t = 2.5$ microns
$Z = 97.7$ ohms

2) $h = 125$ microns $\quad s = 0$
$w = 12.5$ microns $\quad t = 2.5$ microns
$Z = 92.0$ ohms

It is noted that the change in the characteristic impedance is about five percent increase even though the thickness of the added oxide layer is one percent of the substrate height. It is also expected that the glazing of alumina substrate [5] affects the transmission properties in a similar way.

VII. Microstrip Line

A microstrip line is a special case ($\epsilon_3{}^*=1$, $s=0$, $d\to\infty$) of the structure in Fig. 1. Therefore $\tilde{g}(\beta)$ is simplified as

$$\tilde{g}(\beta) = \frac{1}{|\beta| \{1 + \epsilon_1{}^* \coth(|\beta| h)\}}. \tag{25}$$

The line capacitance is obtained by substituting (21), (24), and (25) in (17). The calculated characteristic impedance and the guide wavelength of a sapphire microstrip line are shown, as an example, in Figs. 6, 7, 8, and 9, as indicated by $d/h\to\infty$.

VIII. Potential Distribution

The potential distribution can be evaluated by the inverse Fourier transform,

$$\phi(x, y) = \frac{1}{2\pi}\int_{-\infty}^{\infty} \tilde{\phi}(\beta, y) e^{-j\beta x} d\beta. \tag{26}$$

The potential distribution on the surface of the dielectric sheet gives information to be used in estimating the coupling between two adjacent microstrip lines. Applying (9) in (26),

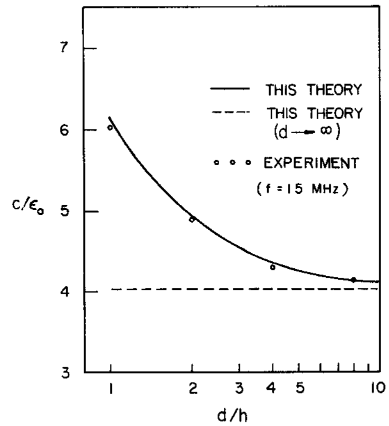

Fig. 3. Comparison of the calculated line capacitance with the measured values. $\epsilon_1^* = \epsilon_3^* = 1$; $\epsilon_2^* = 2.55$ (polystyrene).

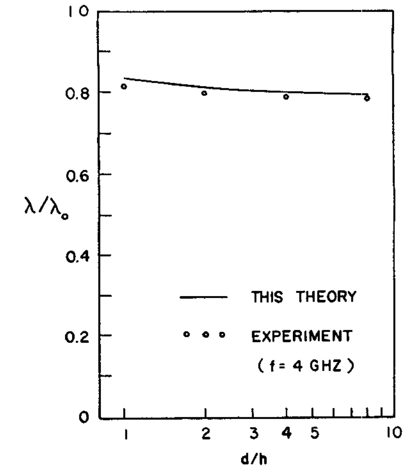

Fig. 4. Comparison of the calculated guide wavelength with the measured values. $\epsilon_1^* = \epsilon_3^* = 1$; $\epsilon_2^* = 2.55$ (polystyrene).

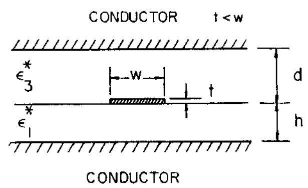

Fig. 5. Shielded microstrip line.

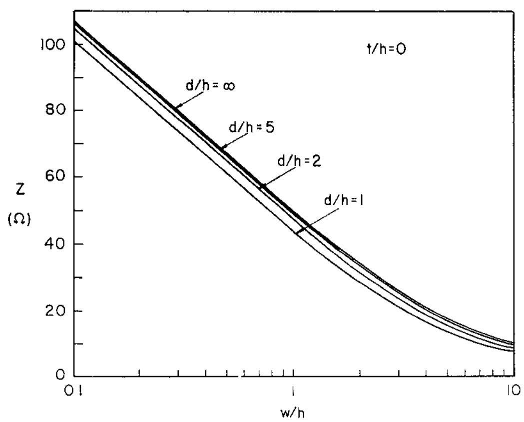

Fig. 6. The calculated characteristic impedance. $\epsilon_1^* = 9.9$ (sapphire); $\epsilon_3^* = 1$; $s = 0$; $t = 0$.

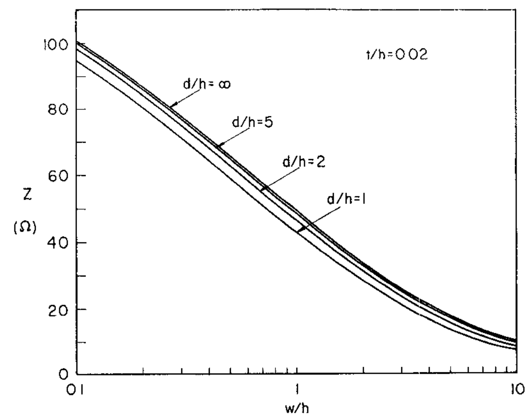

Fig. 7. The calculated characteristic impedance. $\epsilon_1^* = 9.9$ (sapphire); $\epsilon_3^* = 1$; $s = 0$; $t = 0.02h$.

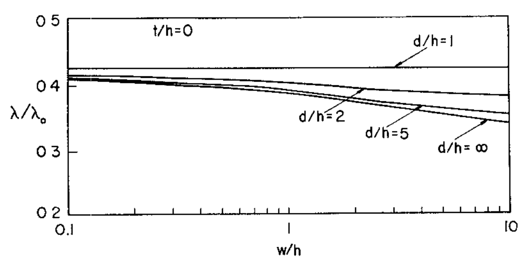

Fig. 8. The calculated guide wavelength. $\epsilon_1^* = 9.9$ (sapphire); $\epsilon_3^* = 1$; $s = 0$; $t = 0$.

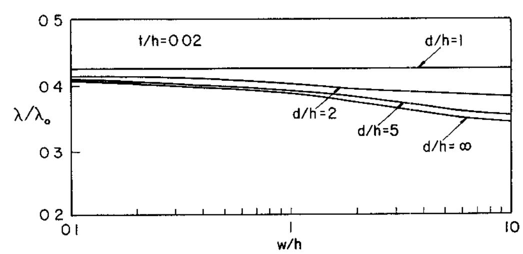

Fig. 9. The calculated guide wavelength. $\epsilon_1^* = 9.9$ (sapphire); $\epsilon_3^* = 1$; $s = 0$; $t = 0.02h$.

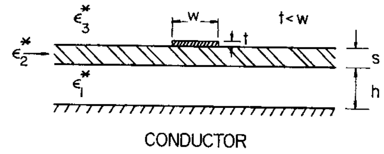

Fig. 10. Double-layer microstrip line.

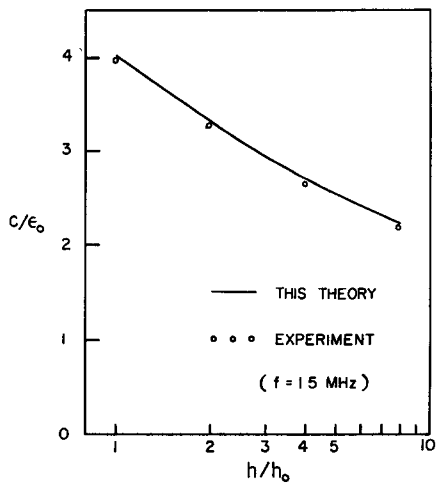

Fig. 11. Comparison of the calculated line capacitance and the measured values. $\epsilon_1^* = \epsilon_3^* = 1$; $\epsilon_2^* = 2.55$ (polystyrene); $d \to \infty$.

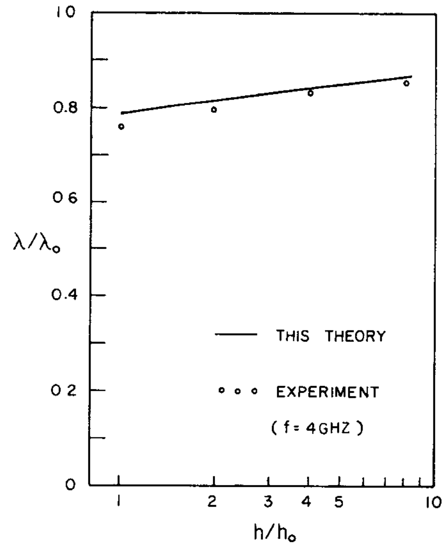

Fig. 12. Comparison of the calculated guide wavelength and the measured values. $\epsilon_1^* = \epsilon_3^* = 1$; $\epsilon_2^* = 2.55$ (polystyrene); $d \to \infty$.

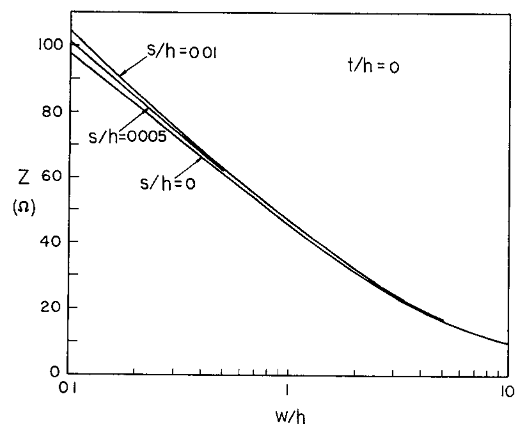

Fig. 13. The calculated characteristic impedance. $\epsilon_1^* = 12$ (Si); $\epsilon_2^* = 4.5$ (SiO); $\epsilon_3^* = 1$; $d \to \infty$; $t = 0$.

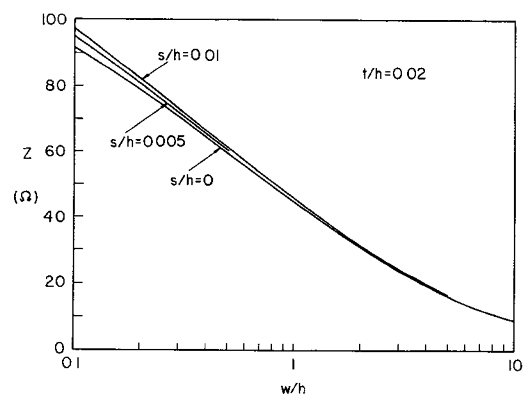

Fig. 14. The calculated characteristic impedance. $\epsilon_1^* = 12$ (Si); $\epsilon_2^* = 4.5$ (SiO); $\epsilon_3^* = 1$; $d \to \infty$; $t = 0.02h$.

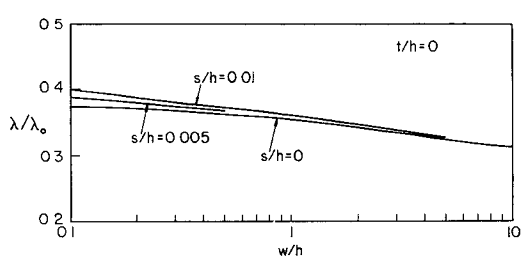

Fig. 15. The calculated guide wavelength. $\epsilon_1^* = 12$ (Si); $\epsilon_2^* = 4.5$ (SiO); $\epsilon_3^* = 1$; $d \to \infty$; $t = 0$.

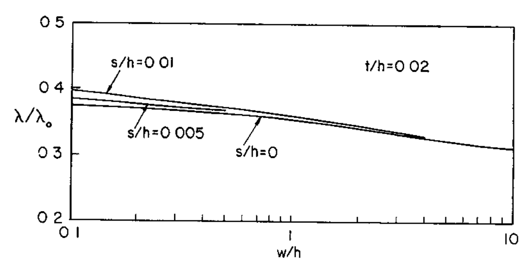

Fig. 16. The calculated guide wavelength. $\epsilon_1^* = 12$ (Si); $\epsilon_2^* = 4.5$ (SiO); $\epsilon_3^* = 1$; $d \to \infty$; $t = 0.02h$.

one obtains this potential:

$$\phi(x, h+s) = \frac{1}{2\pi\epsilon_0}\int_{-\infty}^{\infty}\tilde{f}(\beta)\tilde{g}(\beta)e^{-j\beta x}d\beta. \qquad (27)$$

IX. Discussions

The variational method in the Fourier transformed coordinate was investigated and found to be useful to obtain basic design formulas for microstrip-like transmission lines. By this method, it is possible to take into account all the dielectric boundary conditions no matter how many planar boundaries exist in these lines. The characteristic impedance and the guide wavelength can be obtained for a wide range of structural parameters. The thickness of a thin strip can also be taken into account.

This approach is based on the calculation of the line capacitance by the static field theory, and, therefore, it is an approximation to the electromagnetic theory. One might recall that the conformal mapping and the relaxation method are also the static field theory. However, the analytical treatment of multiple boundaries may be easier by the variational method than by the modified conformal mapping. The computing time seems to be shorter by the variational method than by the relaxation method. At any rate, this variational method can be used within the following limitations.

1) The dielectic layer must be of low loss at the operating wavelength λ_0. This condition is written as $(2\pi\epsilon^* R_d/\eta_0) \gg \lambda_0$, where R_d is the resistivity and $\eta_0 = 120\pi$ ohms.
2) The static field approximation and the nonradiation assumption require $\lambda_0 \gg h+s$.
3) The thin strip approximation requires $t \ll h$ and $t \lesssim w$.

This method may also be applicable to other problems characterized by Poisson's equation, planar geometry, and multiple media. Examples of these problems are

1) the current distribution in multiple resistive media like a planar field-effect transistor,
2) the stationary temperature distribution in a microstrip-like structure with a strip heat source,
3) The wave velocity calculation of a traveling-wave-type electrooptical modulator using a microstrip-like transmission line.

Acknowledgment

The author thanks Prof. R. Mittra for his encouragement and advice, J. Welch for his experimental work.

References

[1] H. A. Wheeler, "Transmission-line properties of parallel strips separated by a dielectric sheet," *IEEE Trans. Microwave Theory and Techniques*, vol. MTT-13, pp. 172–185, March 1965.
[2] K. C. Wolters and P. L. Clar, "Microstrip transmission lines on high dielectric constant substrates for hybrid microwave integrated circuits," presented at the 1967 Internat'l Microwave Symp., Boston, Mass., May 1967, Session V-2.
[3] E. Yamashita and R. Mittra, "Variational method for the analysis of microstrip lines," *IEEE Trans. Microwave Theory and Techniques*, vol. MTT-16, pp. 251–256, April 1968.
[4] H. Guckel and P. A. Brennan, "Picosecond pulse response of interconnections in a common substrate monolithic system," presented at the Internat'l Solid-State Circuits Conf., (Philadelphia, Pa., February 1967), Session XI.
[5] B. T. Vincent, Jr., "Ceramic microstrip for microwave hybrid integrated circuitry," presented at the 1966 Internat'l Microwave Symp., Palo Alto, Calif., May 1966, Session V-2.
[6] H. C. Okean, "Integrated microwave tunnel diode device," presented at the 1966 Internat'l Microwave Symp., Palo Alto, Calif., May 1966, Session V-3.
[7] R. E. Collin, *Field Theory of Guided Waves.* New York: McGraw-Hill, 1960, p. 162.
[8] A. Papoulis, *The Fourier Integral and Its Applications.* New York: McGraw-Hill, 1962.
[9] E. Hallen, *Electromagnetic Theory.* London: Chapman & Hall, 1962, p. 64.
[10] J. M. C. Dukes, "An investigation into some fundamental properties of strip transmission lines with the aid of an electrolytic tank," *Proc. IEE* (London), vol. 103, pt. B, pp. 319–333, May 1956.
[11] S. B. Cohn, "Problems in strip transmission lines," *IRE Trans. Microwave Theory and Techniques*, vol. MTT-3, pp. 119–126, March 1955.
[12] M. Caulton, J. J. Hughes, and H. Sobol, "Measurements on the properties of microstrip transmission lines for microwave integrated circuits," *RCA Rev.*, vol. 27, pp. 377–391, September 1966.